

Intratatumoral Microbiome of Human Primary Liver Cancer

Dingding Qu ,¹ Yi Wang,¹ Qingxin Xia,¹ Jing Chang,^{2,3} Xiangnan Jiang,⁴ and He Zhang¹

Primary liver tumors (PLCs) and liver metastasis currently represent the leading cause of cancer-related deaths worldwide due to poor outcomes, high incidence, and postsurgical recurrence. Hence, novel diagnostic markers and therapeutic strategies for PLCs are urgently needed. The human microbiome can directly or indirectly impact cancer initiation, progression, and response to therapy, including cancer immunotherapy; however, the roles of the microbiota in the tumor microenvironment are not clear and require more investigation. Here, we investigated intratumoral microbial community profiling on formalin-fixed paraffin-embedded tissue samples of patients with PLC by 16S ribosomal RNA using the MiSeq platform. We characterized the microbial communities in different histopathological subtypes and in the different prognoses of patients with PLC. The study revealed microbial population differences not only in carcinoma tissue and the matched adjacent nontumor tissue but in different histopathological subtypes, even in patients with PLC with different prognoses. Interestingly, the abundance of certain bacteria that have antitumor effects at family and genus level, such as *Pseudomonadaceae*, decreased in tumor tissue and was linearly associated with prognosis of patients with PLC. **Conclusion:** We provide a potential novel diagnostic biomarker and therapeutic strategy for early clinical diagnosis and treatment of PLC. (*Hepatology Communications* 2022;6:1741-1752).

Primary liver cancer (PLC) is one of the most fatal malignant tumors in the world. Due to the insidiousness of the onset of PLC and the absence of effective diagnosis markers and treatment methods, the outcomes of PLC are extremely poor and the 5-year average survival rates are extremely low. PLC mainly refers to malignancies that originate from malignant hepatocellular tumors and precursors, such as hepatocellular carcinoma (HCC), which accounts for the majority of PLC, intrahepatic cholangiocarcinoma (iCCA), and combined HCC and iCCA (cHCC-CCA). The main underlying risk factor is liver cirrhosis, predominantly from chronic viral infections (with hepatitis B or C) or alcoholic

liver disease. Due to the lack of specific symptoms and diagnosis markers in early stages, most patients might be diagnosed with early/intermediate-stage disease and treated with curative intent by surgery or receive local ablation or arterially directed therapy for the treatment of embolisms.^(1,2) Therefore, novel diagnostic markers and therapeutic strategies for PLC are urgently needed to improve the outcome of patients with PLC.

Because the human gut microbiota has been commonly considered the most important microecosystem living in symbiosis with the body,⁽³⁻⁵⁾ past studies have focused on serum or fecal microbiota to investigate the links between microbiota metabolism and

Abbreviations: cHCC-CCA, combined hepatocellular carcinoma and intrahepatic cholangiocarcinoma; FFPE, formalin-fixed paraffin-embedded; HCC, hepatocellular carcinoma; iCCA, intrahepatic cholangiocarcinoma; LTS, long-term survivor; OTU, operational taxonomic unit; PCA, principal coordinate analysis; PLC, primary liver cancer; rRNA, ribosomal RNA; STS, short-term survivor.

Received July 22, 2021; accepted January 8, 2022.

Additional Supporting Information may be found at onlinelibrary.wiley.com/doi/10.1002/hep4.1908/supinfo.

Supported by the Nursery Scientific Research Foundation of Affiliated Cancer Hospital of Zhengzhou University (grants to D.D.Q.), the Doctoral Research Initiation Fund of Affiliated Cancer Hospital of Zhengzhou University (grants 3101030102 to H.Z.), and the National Natural Science Foundation of China (grants 31901233 to H.Z.).

© 2022 The Authors. *Hepatology Communications* published by Wiley Periodicals LLC on behalf of American Association for the Study of Liver Diseases. This is an open access article under the terms of the [Creative Commons Attribution-NonCommercial-NoDerivs](https://creativecommons.org/licenses/by-nc-nd/4.0/) License, which permits use and distribution in any medium, provided the original work is properly cited, the use is non-commercial and no modifications or adaptations are made.

View this article online at [wileyonlinelibrary.com](https://onlinelibrary.wiley.com).

DOI 10.1002/hep4.1908

Potential conflict of interest: The authors declare no competing interests.

tumor development. Recent studies have reported that the gut microbiota is different among early HCC, cirrhosis, and healthy controls,⁽⁵⁾ indicating that gut microbiota may act in a crucial role in chronic inflammatory liver diseases and liver cancers. However, few studies have directly explored the potential avenues of crosstalk between tumors and their bacterial counterparts by tumor specimens. Indeed, reports on the microbial characteristics of tumor formalin-fixed paraffin-embedded (FFPE) tissue in clinical patients with PLC are rare.

Numerous, well-characterized, and well-preserved clinical samples are fundamental to explore the specific correlation between the microbiota and disease. FFPE tissue samples are considered consistent with this general principle owing to their routine use and wide availability as clinical materials.⁽⁶⁾ In addition, we chose FFPE tissue samples to investigate the alterations of the tumor microbiome because they are easy to handle, suitable for long-term storage, and can be used in a wide range of molecular applications; most importantly, they can reflect patients' prognosis and survival.⁽⁷⁾ The technique of 16S ribosomal RNA (rRNA) sequencing was found to be more powerful and extensive for the detection of bacteria in FFPE tissue and also relatively economical and practical.⁽⁸⁾ In addition, for 16S rRNA sequence analysis of FFPE tissue flora, reports have been published on gut,⁽⁹⁾ endocarditis,⁽¹⁰⁾ tonsillar tissue,⁽¹¹⁾ and cystic neutrophilic granulomatous mastitis.⁽¹²⁾ To this end, we investigated the intratumoral microbiome on FFPE tissue samples of patients with PLC by 16S rRNA MiSeq sequencing. Results revealed that tumor microbial composition and abundance of certain microbes

were significantly different regardless of whether they were found in tumor and the matched nontumor adjacent tissues or in different histopathological subtypes, even in patients with PLC with different prognoses. Unexpectedly, the relative abundance of *Pseudomonadaceae* at the family and genus level was decreased in tumor tissues and was linearly associated with prognoses of patients with PLC; this may involve the antitumor effect of *Pseudomonadaceae*.⁽¹³⁻¹⁵⁾ In brief, our study revealed intratumoral microbiome differences in various aspects of PLC, including various histopathological subtypes and prognoses, providing a potential novel diagnostic biomarker and therapeutic strategy for patients with PLC.

Participants and Methods

PARTICIPANT INFORMATION

We initially used a discovery cohort of 28 individuals with PLC who required surgery at the Affiliated Tumor Hospital of Zhengzhou University (Henan Province, China) from 2015 to 2016. This cohort included 11 patients with HCC, 8 with iCCA, and 9 with cHCC-CCA. Representative FFPE sections (i.e., at the site of the tumor area) and marginal sections (i.e., nontumor area adjacent to the tumor site) were obtained for all 28 patients. In analysis of the discovery cohort between long-term survivors (LTSs) and short-term survivors (STSs), we compared patients who received surgical resection and who survived more than 5 years after surgery to stage-matched STSs who survived less than 5 years after surgery.

ARTICLE INFORMATION:

From the ¹Department of Pathology, Zhengzhou Key Laboratory of Accurate Pathological Diagnosis of Intractable Tumors, Henan Medical Key Laboratory of Tumor Pathology and Artificial Intelligence Diagnosis, Affiliated Cancer Hospital of Zhengzhou University, Zhengzhou, China; ²School of Life Sciences, Northwestern Polytechnical University, Xi'an, China; ³Medical Service Office, Affiliated Cancer Hospital of Zhengzhou University, Zhengzhou, China; ⁴Department of Pathology, Fudan University Shanghai Cancer Center, Shanghai, China.

ADDRESS CORRESPONDENCE AND REPRINT REQUESTS TO:

He Zhang, Ph.D.
Department of Pathology, Affiliated Cancer Hospital of
Zhengzhou University

127th Dongming Rd., Zhengzhou 450000, Henan, China
E-mail: zlyzhanghe4202@zzu.edu.cn
Tel.: +86 0371-65587018

This study was approved by the Institutional Review Board of the Affiliated Cancer Hospital of Zhengzhou University and was performed in accordance with the Helsinki Declaration and rules of good clinical practice. All participants signed written informed consents after the study protocol was fully explained and signed an informed consent agreeing to deliver their own anonymous information for future studies.

HISTOLOGY

Intact surgical specimens were delivered to our pathology laboratory under sterile conditions. Pickup was followed by fixation of samples in 10% neutral buffered formalin and processed for paraffin embedding. Histology sections were cut at 3–5 μm and stained with hematoxylin and eosin. A medium-capacity digital slide scanner (Pannoramic Scan; 3DHISTECH Ltd., Hungary) was used for imaging histology sections, and all images were taken at magnification $\times 2$ or $\times 5$. Representative images were captured from every sample to demonstrate the tumor area and the matched adjacent nontumor area.

FFPE SAMPLE COLLECTION AND DNA EXTRACTION

For each sample, the first few scrolls from the FFPE blocks were discarded; then, two 2-mm holes were drilled at the tumor site and at the matched adjacent tissues and the drillings placed into sterile 2-mL centrifuge tubes. This drill-hole method in FFPE tissues was based on information from a relevant publication⁽¹⁶⁾ with some necessary improvements. The sampling process was performed on a clean bench, and the drill-hole tool was prepped with 75% alcohol before and after drilling. The main protocols and sterilization operations are shown in Supporting Fig. S2. The surgical specimens from the liver cancer tissue were sufficient to extract enough DNA for 16S rRNA sequencing, and the drill-hole method maintained a relatively high level of DNA concentration and purity (as shown in Supporting Table S1). Microbial total DNA from the FFPE tissue was extracted using the QIAamp DNA FFPE tissue kit (QIAGEN, CA) according to the manufacturer's protocol. Samples were then immediately frozen and stored at -20°C until used for the experiment. A NanoDrop ND-1000

Spectrophotometer (Nucliber) was used for DNA quantification with an equivalent of 1 μL of each sample at room temperature.

POLYMERASE CHAIN REACTION AMPLIFICATION, MISEQ SEQUENCING, AND SEQUENCE DATA PROCESS

Extracted DNA samples were amplified, DNA libraries were constructed, and sequencing was performed on an Illumina MiSeq platform by Shanghai Majorbio Bio-Pharm Technology Co., Ltd., China. The 16S rRNA gene sequencing methods were adapted from the methods developed for the Earth Microbiome Project(X) and the National Institutes of Health Human Microbiome Project (HMP).^(17–19) In brief, the bacterial 16S rRNA gene V4 region was amplified from the diluted DNA extracts with the primers 515 forward (5'-GTGCCAGCMGCCGCGTAA-3') and 806 reverse (5'-GGACTACHVGGGTWTCTAAT-3').⁽¹⁹⁾ After purification and quantification of the polymerase chain reaction (PCR) products, the sample was equimolar mixed. Parallel tagged sequencing was performed with sequencing of the 2×250 -base pair cartridges in the Illumina MiSeq platform (Illumina, CA). Read pairs were demultiplexed based on unique molecular barcodes added by PCR during library generation, then merged using USEARCH v7.0.1090.⁽²⁰⁾

BIOINFORMATICS ANALYSIS

We randomly chose the reads from all samples with equal number, and operational taxonomic units (OTUs) were binned by the UPARSE pipeline.⁽²¹⁾ Performance of the UPARSE pipeline was evaluated and compared with that reported for samples of the HMP data set. Merging allowed zero mismatches and a minimum overlap of 50 bases, and merged reads were trimmed at the first base with a Phred score (Q) ≤ 5 . A quality filter was applied to the resulting merged reads, and those containing above 0.5% expected errors were discarded. Sets of sequences with at least 97% identified were defined as an OTU, and chimeric sequences were identified and removed using Uchime.⁽²¹⁾ The taxonomy of each 16S rRNA gene sequence was analyzed using RDP Classifier (<http://rdp.cme.msu.edu/>) against the SILVA ribosomal RNA gene database using a confidence threshold of 70%.⁽²²⁾ Rarefaction curves were

plotted for each sample to determine the abundance of communities and sequencing data of each sample.⁽²³⁾ Bacterial diversity was determined by sampling-based OTU analysis and presented by the Shannon index, Simpson index, and Chao index, which were calculated using the R program package *vegan*.⁽²⁴⁾ Beta diversity was assessed by unweighted and weighted UniFrac distance matrices and visualized by principal coordinate analysis (PCA), controlled by 10^3 jackknife replicates.⁽²⁵⁾ PCA was conducted using the R package (<http://www.R-project.org/>) to display microbiome space between samples. The weighted and unweighted UniFrac distances were calculated with the *phyloseq* package.⁽²⁶⁾ Statistically significant differences in the relative abundance of taxa associated with groups of patients were determined using linear discriminant analysis (LDA) effect size (<http://huttenhower.sph.harvard.edu/lefse/>).⁽²⁷⁾ Only taxa with LDA > 4 at $P < 0.05$ were considered significantly enriched.

STATISTICAL ANALYSIS

SPSS V.21.0 for Windows (SPSS, Chicago, IL) was used for all statistical analyses. One-way analysis of variance was used to evaluate differences among the three groups. Continuous variables were compared using the Wilcoxon rank sum test between both groups. Fisher's exact test compared categorical variables. $P < 0.05$ indicated a statistically significant result.

Results

CLINICAL CHARACTERISTICS OF PATIENTS AND FFPE SAMPLE

After strict inclusion and exclusion criteria, this study finally enrolled 28 patients with PLC from the Affiliated Tumor Hospital of Zhengzhou University, Henan Province. Clinical characteristics of the participants in the discovery cohort, including age, sex, and medical history according to different pathological subtypes of PLC, are listed in [Table 1](#), and the distribution of the above indexes did not differ ($P > 0.05$). FFPE samples were obtained from surgical resection tissues of patients with PLC. Specimens were postoperatively staged by a dedicated pathologist according to the tumor, node, and metastasis (TNM) staging system⁽²⁸⁾ and American Joint Committee on Cancer

stage groupings (I-IV). Matched tumoral and paratumoral areas were isolated from each FFPE peripheral zone of the PLC tissue samples with different pathological subtypes ([Fig. 1](#)). When more tumoral foci were present, the more representative tumoral area was selected based on the highest grade.

ABUNDANCE OF CERTAIN MICROBES ALTERED IN THE TUMOR MICROENVIRONMENT

To investigate the intratumoral microbiome of patients with PLC, we compared alpha diversity between the tumor and the matched adjacent nontumor tissues of FFPE samples. We found that microbial diversity, as estimated by the Sobs index, Chao index, Shannon index, and Simpson index, had nonsignificant differences in tumor tissues ([Fig. 2A](#)). A Venn diagram displaying the overlap between groups showed that 588 of the total 1,075 OTUs were shared between the groups ([Fig. 2B](#)). Notably, 209 of 1,075 OTUs were unique for PLC. We then calculated beta diversity using unweighted UniFrac. PCA indicated a symmetrical distribution of the tumor-microbial community among all samples ([Fig. 2C](#)). To identify key OTU phylotypes in tumor tissues of patients with PLC, OTU abundances were analyzed by the Wilcoxon rank-sum test, using the Benjamini-Hochberg method. Results showed that bacterial phyla of *Proteobacteria*, *Actinobacteria*, *Bacteroidetes*, and *Firmicutes*, together accounting for up to 90% of sequences on average, were the four dominant populations in both tumor and the matched adjacent nontumor tissues ([Fig. 2D](#)). Average composition of the bacterial community at the genus level is shown in [Fig. 2E](#). Unexpectedly, at the family or genera level, *Pseudomonas* was significantly decreased in tumor tissues, which might be due to its antitumor effects ([Fig. 2G,I](#)). Conversely, *Rhizobiaceae* at the family level and *Agrobacterium* at the genus level were significantly increased in tumor tissues ([Fig. 2F,H](#)).

MICROBIAL SIGNATURES REVEAL SIGNIFICANT CORRELATION WITH PROGNOSIS

To further explore the role of intratumoral microbial composition in mediating clinical outcomes of patients with PLC, we then compared alpha and beta diversities between long- and short-term survivor

TABLE 1. CLINICOPATHOLOGICAL CHARACTERISTICS OF ALL PARTICIPANTS

Clinical and Pathological Indexes	HCC (n = 11)	ICC (n = 8)	cHCC-ICC (n = 9)	PValue
Age, years, median (range)	53.9 (37-67)	59.3 (50-74)	52 (33-66)	0.31
Sex (male/female)	6/5	3/5	8/1	0.08
Surgery date	Jan 2015-June 2015	Mar 2015-Apr 2016	Feb 2015-Sept 2016	
Postoperative survival, months, mean \pm SD	37.00 \pm 23.82	22.88 \pm 17.22	21.67 \pm 17.52	0.19
Hepatitis B, number	10	2	4	0.01
Liver cirrhosis, number	0	2	3	0.13
Lymphatic metastasis, number	1	3	1	0.23

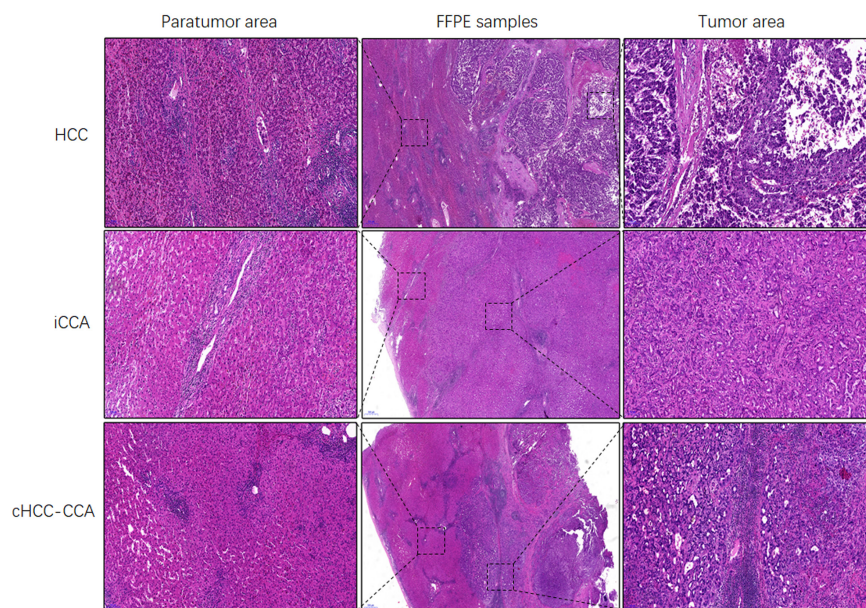


FIG. 1. Histology of representative sections of tumor area (right, magnification $\times 5$) and the matched adjacent nontumor area (left, magnification $\times 5$) from different histopathological subtypes of PLC. The area plotted by the black dotted boxes in the middle column (magnification $\times 2$) show the drillings for microbiome sequencing analysis.

groups and again revealed distinct tumoral microbiome profiles. We used a discovery cohort to compare patients who were surgically resected and who survived more than 5 years after surgery (LTS) to stage-matched STSs who survived less than 5 years after surgery.⁽²⁹⁾ Analysis of beta diversity based on unweighted UniFrac distances showed that the microbiome of the LTS group was distinct from that of the STS group ($P = 0.05$; Fig. 3A), but alpha diversity between the two groups was nonsignificant (Supporting Fig. S2A). The key OTU phylotypes were analyzed using the Wilcoxon rank-sum test with the Benjamini-Hochberg method. The dominant

populations of phyla were consistent with tumor-adjacent pairs (Supporting Fig. S2B). The average composition of the bacterial community at the genus level is shown in Supporting Fig. S2C. In addition, Pearson correlation analyses across groups revealed a positive correlation between prognosis development of patients with PLC and relative abundance increase of *Pseudomonas* at the family and genus levels (Supporting Fig. 3B,C). At the family and genus levels, the Wilcoxon rank-sum test revealed a significant difference in the proportions of *Pseudomonas* between the two groups, indicating *Pseudomonas* as a critical factor influencing prognosis of patients with

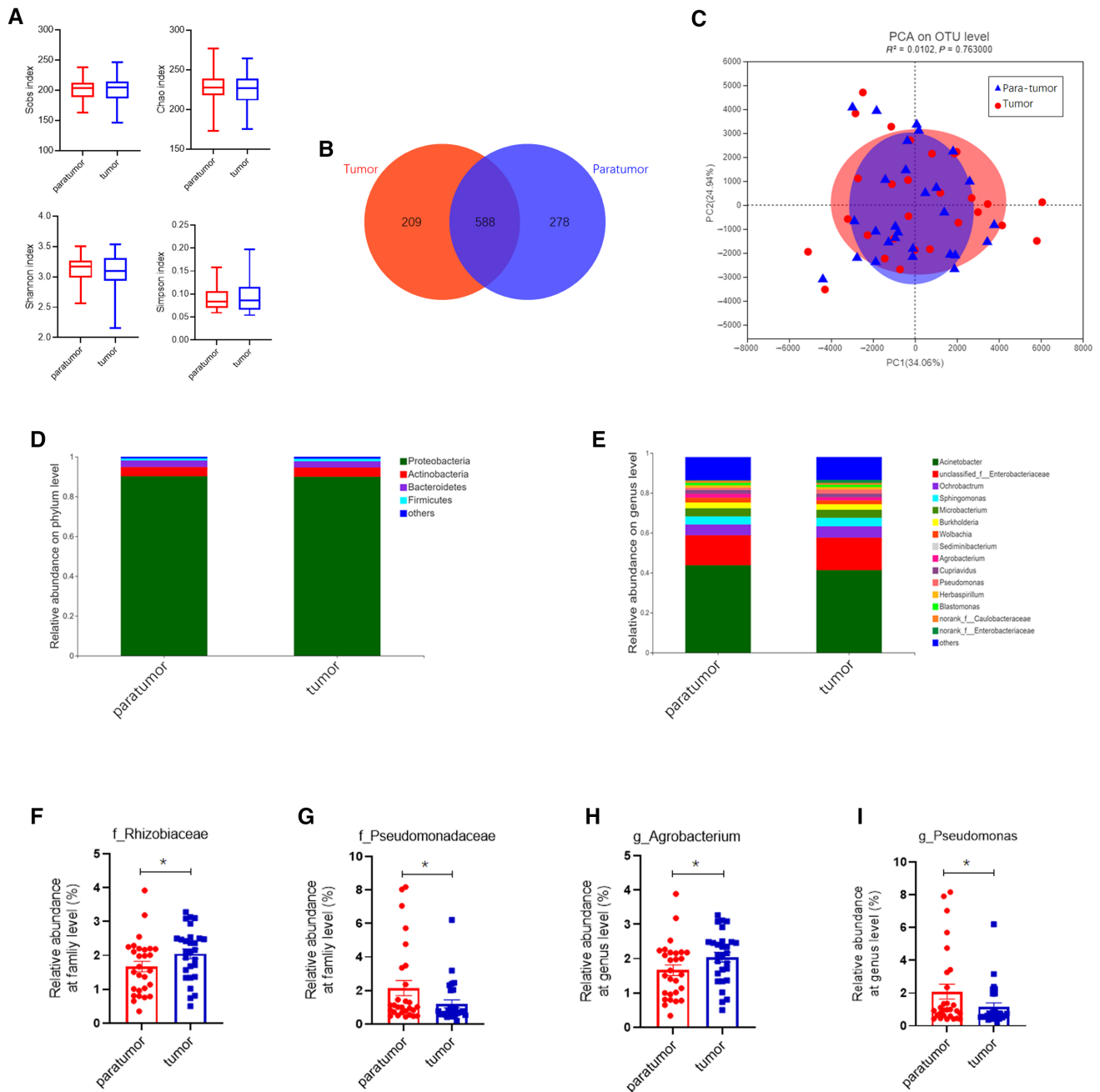


FIG. 2. Microbiota profiles between tumor tissues and the matched adjacent nontumor tissues. (A) Microbial diversity estimated by the Sobs index, Chao index, Shannon index, and Simpson index in samples of each group of patients. (B) Venn diagram displaying the degree of overlap of bacterial OTUs between the tumor and paratumor groups. (C) PCA of bacterial beta diversity based on unweighted UniFrac distances. Composition of microbiota at the (D) phylum level and (E) genus level between the two groups. (F-I) The increased microbial community at the (F) family level and (H) genus level and the decreased microbial community at the family level (G) and genus level (I) in tumor tissues versus the matched paratumor tissues. Values in (A) and (F-I) are expressed as mean (box) ± SEM; **P* < 0.05, paired *t* test). Abbreviations: f, family; g, genus.

PLC (Fig. 3D,E). Furthermore, to identify the most relevant taxa responsible for the differences between clinical prognoses, we conducted high-dimensional

class comparisons using liner discriminant analysis of effect size analysis,⁽²⁷⁾ which detected marked differences in the predominance of bacterial

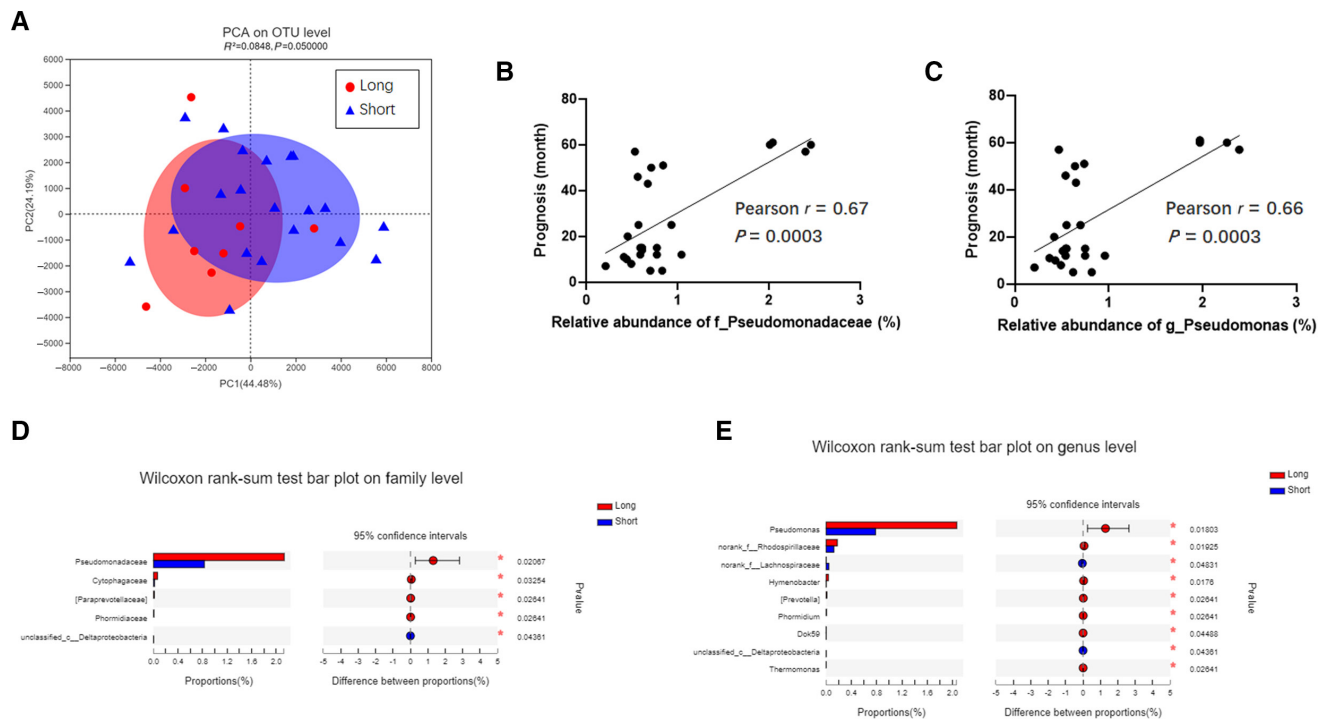


FIG. 3. The intratumoral microbiota profile differs in LTSs (red) and STSs (blue). (A) Beta diversity was calculated using the unweighted UniFrac by PCA; this indicated a symmetrical distribution of the tumor microbial community between the LTS and STS groups ($P = 0.050$). Pearson correlation between prognosis development and relative abundance of *Pseudomonas* at the (B) family and (C) genus levels in patients with PLC ($P = 0.0003$, $P = 0.0003$, respectively). Significantly altered intratumoral microbiota between the LTS and STS groups at (D) family and (E) genus levels was indicated by the Wilcoxon rank-sum test. Abbreviations: f, family; g, genus.

communities between LTSs and STSs (Supporting Fig. S2D,E). LTS tumors exhibited a predominance of *Pseudomonas*, *Thermomonas*, *Paraprevotellaceae*, and other bacteria at the family or genus level. In contrast, the PLC STS cases were dominated by *Enhydrobater*, *Lachnospiraceae*, and *Deltaproteobacteria* at the matched level (Supporting Fig. S2D,E). Results obtained from all these approaches confirmed the underlying critical communications between microbiota in the tumor microenvironment and clinical prognosis.

DIFFERENT PATHOLOGICAL SUBTYPES OF PLC HAVE A DISTINCT MICROBIAL COMPOSITION

For characterization of the microbiome associated with different histopathological subtypes of PLC, we then compared alpha diversity among the HCC,

iCCA, and cHCC-CCA groups. We found a significant decrease in bacterial richness cHCC-CCA and a nonsignificant difference between HCC and iCCA (Fig. 4A). The number and identity of shared OTUs were evaluated through a Venn diagram. Overlap between groups showed that 295 of the total 797 OTUs were shared among the three groups (Fig. 4B); 80 of 458 OTUs were unique for the cHCC-CCA group, and the OTU number was significantly lower than the HCC and iCCA groups. To display microbiome space between samples, beta diversity was calculated using weighted UniFrac, and PCA analysis indicated a symmetrical distribution of tumor microbial community among all samples of different histopathological subtypes of PLC (Fig. 4C). Results revealed that the microbiome of the HCC group was significantly different from that of the iCCA and cHCC-CCA groups (analysis of similarities all $r^2 = 0.156$, $P = 0.024$).

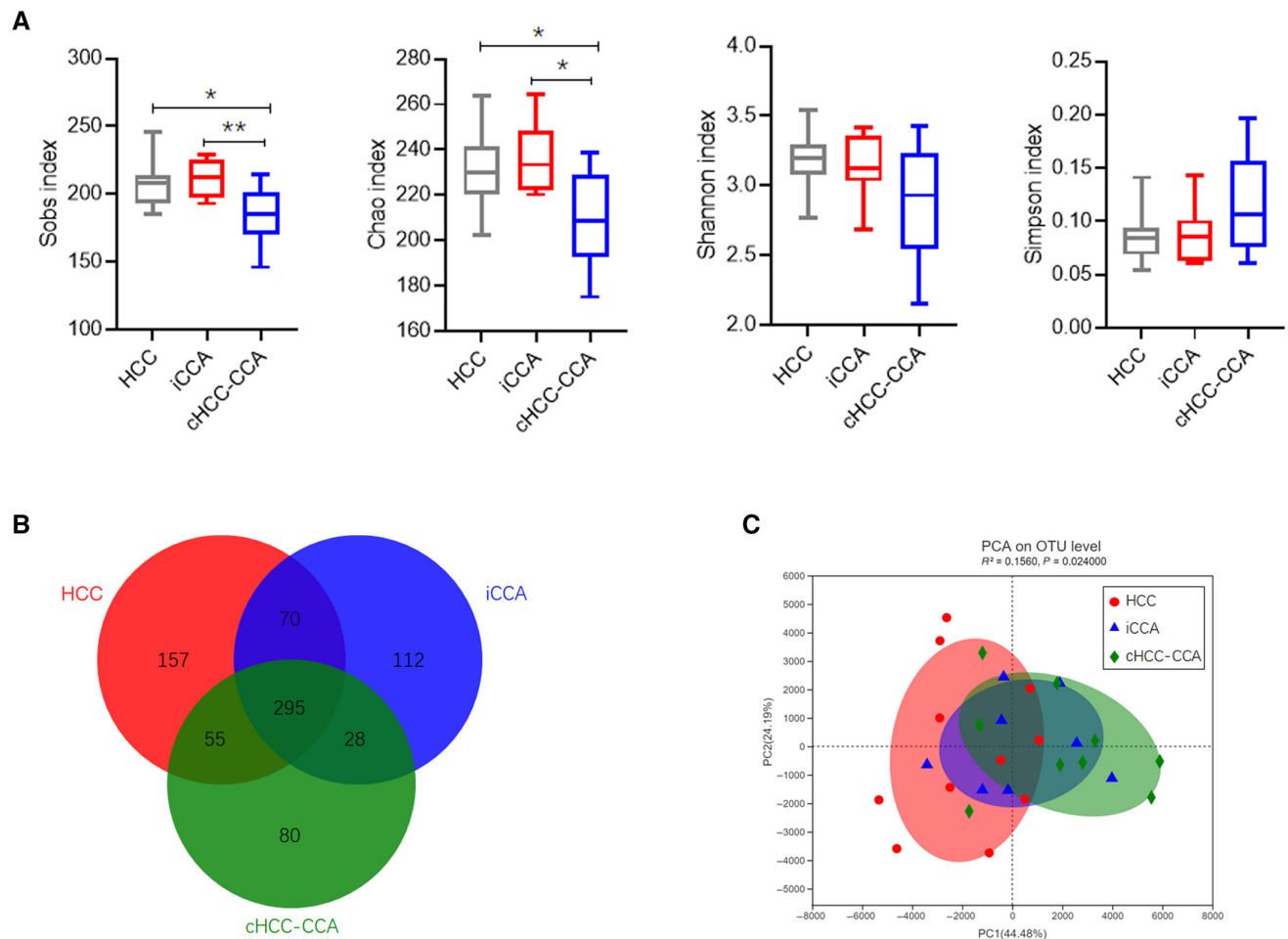


FIG. 4. Intratumoral microbial diversity in different histopathological subtypes of PLC. (A) Microbial alpha-diversity estimated by the Sobs index, Chao index, Shannon index, and Simpson index in samples of each group of patients (* $P < 0.05$, ** $P < 0.01$). (B) Venn diagram displaying the overlap between groups showed that 295 of the total richness of 797 OTUs were shared among the three groups, while only 80 of 458 OTUs were unique for the cHCC-CCA group. (C) PCA of bacterial beta diversity based on unweighted UniFrac distances among the three groups.

PHYLOGENETIC PROFILES OF TUMOR MICROBIAL COMMUNITIES IN DIFFERENT HISTOPATHOLOGICAL SUBTYPES OF PLC

Phylotypes with a median relative abundance larger than 0.01% of total abundance were included for comparison, and the key OTU phylotypes were analyzed using the Wilcoxon rank-sum test with the Benjamini-Hochberg method. Bacterial phyla of *Proteobacteria*, *Actinobacteria*, *Bacteroidetes*, and *Firmicutes*, together accounting for up to 90% of sequences on average, were the four dominant populations in three groups (Fig.

5A). Average composition of the bacterial community of dominant populations at the genus level is shown in Fig. 5B. Analysis by the Wilcoxon rank-sum test screened out the bacteria whose mean proportion difference was most striking at the family and genus levels. Results suggested that the bacterial community with the highest mean proportions were all *Enterobacteriaceae* species at the family and genus levels among the three different histopathological subtypes of PLC. Compared with the iCCA and cHCC-CCA groups, the mean proportions of *Enterobacteriaceae* at the family level were significantly increased in HCC (by up to 10%; $P = 0.0132$), but there was a nonsignificant difference between iCCA and cHCC-CCA (Fig. 5C). In contrast, the mean

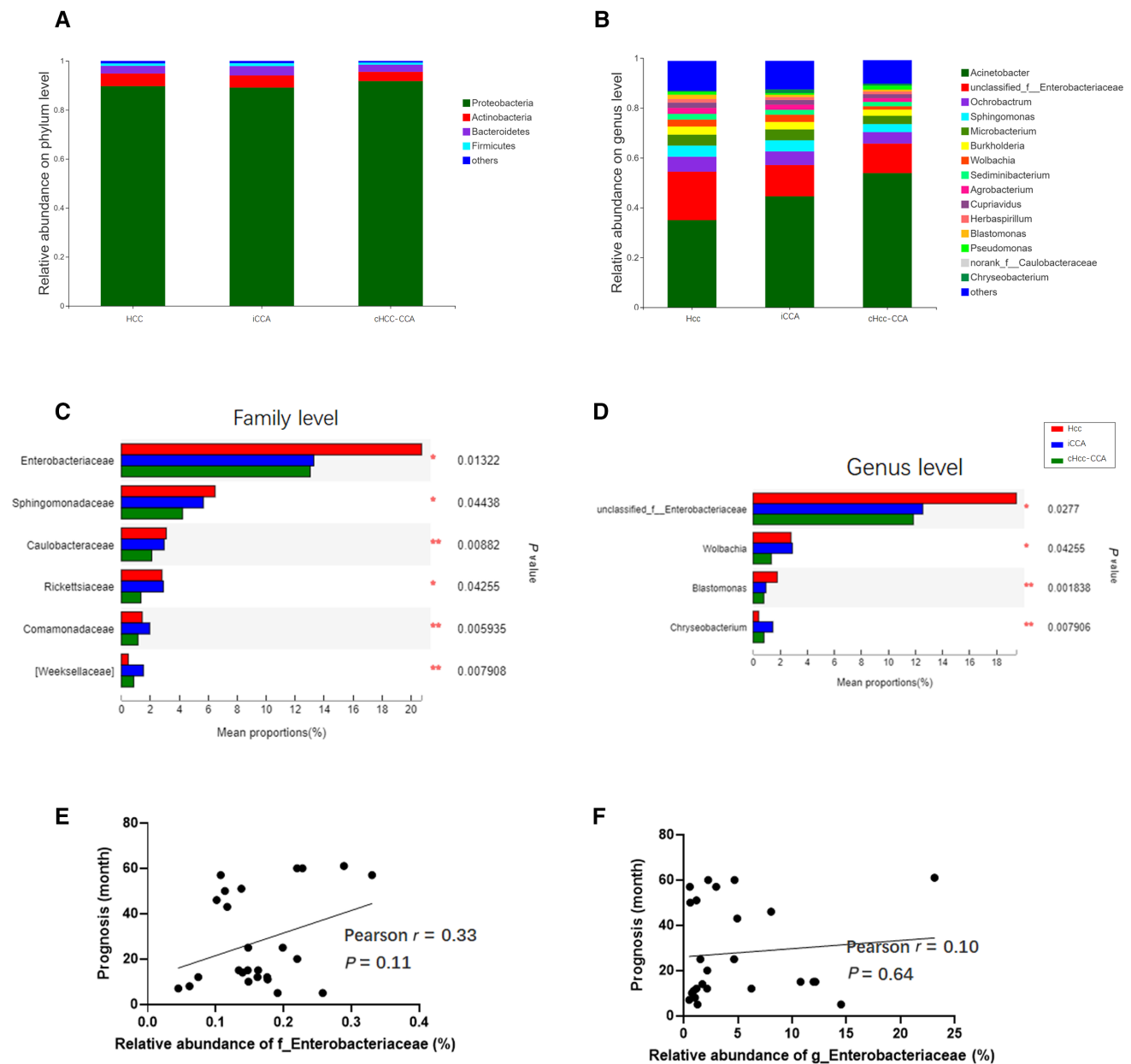


FIG. 5. Phylogenetic profiles of intratumoral microbes among patients with HCC ($n = 11$), patients with iCCA ($n = 8$), and patients with cHCC-CCA ($n = 9$). Composition of tumor microbiota at the (A) phylum level and (B) genus level among the three groups. Significantly altered intratumoral microbiota among the three groups at the (C) family and (D) genus levels was shown by the Wilcoxon rank-sum test. Pearson correlation between prognosis development and relative abundance of *Enterobacteriaceae* at the (E) family and (F) genus levels of patients with PLC ($P = 0.11$, $P = 0.64$, respectively). Abbreviations: f, family; g, genus.

proportions of *Caulobacteraceae* and *Rickettsiaceae* at the family level were significantly decreased in the cHCC-CCA group (all $P < 0.05$). Correspondingly, the mean proportions of *Enterobacteriaceae* and *Blastomonas* at the family and genus levels were significantly increased in HCC, but the mean proportion of *Wolbachia* was

significantly decreased in cHCC-CCA (all $P < 0.05$; Fig. 5D). However, Pearson correlation analyses across groups revealed that the relative abundance of *Enterobacteriaceae* was not significantly correlated with the prognosis of patients with PLC at the family and genus levels (Fig. 5E,F).

Discussion

Symbiotic relationships between human and microbes have been studied for many years, and the concept of the gut microbiome serving as a tool toward targeted noninvasive biomarkers for specific diseases or cancer has been established by compelling studies. Previous studies on PLC from a microbial angle were mainly to investigate the interrelations between gut microbiota and PLC through the gut–liver axis. However, this indirect research has limitations and low concordance, which is a pervasive challenge that limits the capacity to identify causal relationships between host-associated microorganisms and pathology.^(30,31) Researchers suggest that human participants with a disease vary from healthy controls in critical microbiota-associated variables that confound microbiota analyses to produce spurious microbial associations with human diseases.⁽³⁰⁾ In addition, recent studies that have examined the role of microbiota in human tumors through postoperative specimens or serum samples can directly reflect the tumor microbial characteristics but cannot be effectively linked to prognosis.^(32–35) Compared to the gut microbiome, postoperative specimens, and serum samples, pathological FFPE tissue samples have the advantages of a long preservation time and enabling retrospective analysis at any time. Thus, FFPE samples represent the largest collection of patient material and are currently recognized as a viable source material for bacterial analysis.^(11,36)

The microbiota can exert regulatory effects in other sites beyond the gut. In this study, we have characterized for the first time the tumor microbiome of FFPE samples from patients with PLC with different prognoses and different histopathological subtypes by using 16S rRNA MiSeq sequencing. We found that microbial diversities, including alpha and beta diversity, and the dominant populations have nonsignificant differences between tumor tissues and the matched adjacent nontumor tissues; this may be attributed to their homogeneous microenvironment. Interestingly, some specific bacteria that have antitumor effects, such as *Pseudomonadaceae*, were significantly decreased in tumor areas of the FFPE samples and were positively and linearly associated with the prognosis of patients with PLC. Furthermore, the microbial diversities were significantly different between LTS and STS groups. This indicates that an altered or “dysbiotic”⁽³⁷⁾ tumor

microbiota may be involved in a poor prognosis. In clinical applications, *Pseudomonas aeruginosa* injection, made from an inactivated mutant strain of *P. aeruginosa* (PA-MSHA), recently has become a type of therapeutic biological product approved in China for adjuvant treatment of patients with malignant tumors.^(38–40)

Our study represents the first report to explore the influence of the intratumoral microbiota on different histopathological subtypes of PLC through FFPE samples. PLC mainly refers to malignancies that originate from HCC, which accounts for the majority of PLCs, iCCA, and cHCC-CCA, and the three PLC subtypes are significantly different in terms of pathogenesis, biological behavior, histological morphology, treatment, and prognosis. Traditional morphopathology primarily emphasizes qualitative diagnosis of PLC, which is not sufficient to resolve the major concern of increasing the long-term treatment efficacy of PLC in clinical management.⁽⁴¹⁾ Therefore, it is necessary to establish a novel microbial typing system specific for PLC. In our study, a total of 28 FFPE samples from different histopathological subtypes of PLC were selected and analyzed using 16S rRNA MiSeq sequencing. The results displayed a significant decrease in alpha diversity and unique OTUs in cHCC-CCA groups, accompanied by lower species diversity, richness, and evenness of microbial communities. Results indicated a significant global shift in intertumoral microbiota from a single-type tumor to combined tumor, and the altered microbial community might play an important role during cHCC-CCA initiation and development. Notably, analysis of beta diversity showed there were close correlations between the microbiome profiles of the iCCA and cHCC-CCA groups compared with the HCC group and that the HCC group exhibited unique bacterial biomarkers, such as *Enterobacteriaceae*. The result of the PCA analysis is consistent with the World Health Organization classification of digestive system tumors,⁽⁴²⁾ which differs slightly from an earlier classification⁽⁴³⁾ in that iCCA and cHCC-CCA are now included within the category of malignant biliary tumors; this distinguishes those diseases from HCC, which is categorized as malignant hepatocellular tumors.⁽⁴⁴⁾ cHCC-CCA is defined as a PLC showing unequivocal presence of both hepatocytic and cholangiocytic differentiation in the same tumor;

the two components histologically can either be juxtaposed with or intermingled with each other.⁽⁴⁵⁾ A previous study demonstrated that the genetics of cHCC-CCA was closer to iCCA than HCC.⁽⁴⁶⁾ Indeed, the PCA analysis of the tumor microbiome in our study displayed consistent findings and is the first report to classify the different subtypes of PLC by their respective intratumoral microbial characteristics. Based on the discovered microbial biomarkers, patients with PLC could be classified with high sensitivity and specificity.

Although our study is limited by its retrospective nature and the absence of healthy controls for comparison, our findings have sufficiently illustrated the intratumoral microbial characteristics and crucial bacterial candidates that contribute to tumor development in the different prognoses and histopathological subtypes of PLC. The discriminatory power of these candidate biomarkers paves the way for establishing intratumoral microbiome tests for clinical diagnostic and prognostic screening for PLC. Thus, we propose that intratumoral microbiota-targeted biomarkers may become a potential noninvasive tool for the pathological diagnosis of PLC. Additional large cohort studies are needed to determine chronological order and to evaluate microbial characteristic changes in patients with PLC. The cross-sectional nature of the present study prevented us from elucidating the mechanisms and longitudinal view of relevance. Ultimately, understanding the intratumoral microbiota dynamics of liver carcinogenesis and development may provide novel diagnostic biomarkers and improve the prognosis for PLC.

REFERENCES

- 1) Dawkins J, Webster RM. The hepatocellular carcinoma market. *Nat Rev Drug Discovery* 2019;18:13-14.
- 2) Forner A, Reig M, Bruix J. Hepatocellular carcinoma. *Lancet* 2018;391:1301-1314.
- 3) Eckburg PB, Bik EM, Bernstein CN, Purdom E, Dethlefsen L, Sargent M, et al. Diversity of the human intestinal microbial flora. *Science* 2005;308:1635-1638.
- 4) Cani PD, Delzenne NM. The role of the gut microbiota in energy metabolism and metabolic disease. *Curr Pharm Design* 2009;15:1546-1558.
- 5) Ren Z, Li A, Jiang J, Zhou L, Yu Z, Lu H, et al. Gut microbiome analysis as a tool towards targeted non-invasive biomarkers for early hepatocellular carcinoma. *Gut* 2019;68:1014-1023.
- 6) Blow N. Tissue preparation: tissue issues. *Nature* 2007;448:959-963.
- 7) Robbe P, Popitsch N, Knight SJL, Antoniou P, Becq J, He M, et al.; 100,000 Genomes Project. Clinical whole-genome sequencing from routine formalin-fixed, paraffin-embedded specimens: pilot study for the 100,000 Genomes Project. *Genet Med* 2018;20:1196-1205.
- 8) Racsá LD, DeLeon-Carnes M, Hiskey M, Guarner J. Identification of bacterial pathogens from formalin-fixed, paraffin-embedded tissues by using 16S sequencing: retrospective correlation of results to clinicians' responses. *Hum Pathol* 2017;59:132-138.
- 9) Stewart CJ, Fatemizadeh R, Parsons P, Lamb CA, Shady DA, Petrosino JF, et al. Using formalin fixed paraffin embedded tissue to characterize the preterm gut microbiota in necrotising enterocolitis and spontaneous isolated perforation using marginal and diseased tissue. *BMC Microbiol* 2019;19:52.
- 10) Solomon IH, Lin C, Horback KL, Kanjilal S, Rojas-Rudilla V, Brigl M, et al. Utility of histologic and histochemical screening for 16s ribosomal RNA gene sequencing of formalin-fixed, paraffin-embedded issue for bacterial endocarditis. *Am J Clin Pathol* 2019;152:431-437.
- 11) Zhu A, Yang X, Bai L, Hou Y, Guo C, Zhao D, et al. Analysis of microbial changes in the tonsillar formalin-fixed paraffin-embedded tissue of Chinese patients with IgA nephropathy. *Pathol Res Pract* 2020;216:153174.
- 12) Naik MA, Korlimarla A, Shetty ST, Fernandes AM, Pai SA. Cystic neutrophilic granulomatous mastitis: a clinicopathological study with 16s rRNA sequencing for the detection of corynebacteria in formalin-fixed paraffin-embedded tissue. *Int J Surg Pathol* 2020;28:371-381.
- 13) Tahmourespour A, Ahmadi A, Fesharaki M. The anti-tumor activity of exopolysaccharides from *Pseudomonas* strains against HT-29 colorectal cancer cell line. *Int J Biol Macromol* 2020;149:1072-1076.
- 14) Leshem Y, Pastan I. *Pseudomonas* exotoxin immunotoxins and anti-tumor immunity: from observations at the patient's bedside to evaluation in preclinical models. *Toxins (Basel)* 2019;11:20.
- 15) Zhang L, Liu M, Jamil S, Han R, Xu G, Ni Y. PEGylation and pharmacological characterization of a potential anti-tumor drug, an engineered arginine deiminase originated from *Pseudomonas plecoglossicida*. *Cancer Lett* 2015;357:346-354.
- 16) Cavarretta I, Ferrarese R, Cazzaniga W, Saita D, Luciano R, Carerola ER, et al. The microbiome of the prostate tumor microenvironment. *Eur Urol* 2017;72:625-631.
- 17) Human Microbiome Project Consortium. A framework for human microbiome research. *Nature*. 2012;486:215-221.
- 18) Human Microbiome Project Consortium. Structure, function and diversity of the healthy human microbiome. *Nature*. 2012;486:207-214.
- 19) Caporaso JG, Lauber CL, Walters WA, Berg-Lyons D, Huntley J, Fierer N, et al. Ultra-high-throughput microbial community analysis on the Illumina HiSeq and MiSeq platforms. *ISME J* 2012;6:1621-1624.
- 20) Edgar RC. Search and clustering orders of magnitude faster than BLAST. *Bioinformatics* 2010;26:2460-2461.
- 21) Edgar RC. UPPARSE: highly accurate OTU sequences from microbial amplicon reads. *Nat Methods* 2013;10:996-998.
- 22) Quast C, Pruesse E, Yilmaz P, Gerken J, Schweer T, Yarza P, et al. The SILVA ribosomal RNA gene database project: improved data processing and web-based tools. *Nucleic Acids Res* 2013;41:D590-D596.
- 23) Amato KR, Yeoman CJ, Kent A, Righini N, Carbonero F, Estrada A, et al. Habitat degradation impacts black howler monkey (*Alouatta pigra*) gastrointestinal microbiomes. *ISME J* 2013;7:1344-1353.
- 24) Oksanen J, Blanchet FG, Friendly M, Kindt R, Legendre P, McGlinn D, et al. *vegan: Community Ecology Package*. Ordination methods, diversity analysis and other functions for community and vegetation ecologists, Version 2.5-1. Comprehensive R Archive Network; 2018. https://www.researchgate.net/publication/324693493_vegan_Community_Ecolo

- [gy_Package_Ordination_methods_diversity_analysis_and_other_functions_for_community_and_vegetation_ecologists_Version_25-1_URL_httpsCRANR-projectorgpackagevegan..](https://CRAN.R-project.org/package=vegan)
- 25) DeSantis TZ, Hugenholtz P, Larsen N, Rojas M, Brodie EL, Keller K, et al. Greengenes, a chimera-checked 16S rRNA gene database and workbench compatible with ARB. *Appl Environ Microbiol* 2006;72:5069-5072.
 - 26) McMurdie PJ, Holmes S. phyloseq: an R package for reproducible interactive analysis and graphics of microbiome census data. *PLoS One* 2013;8:e61217.
 - 27) Segata N, Izard J, Waldron L, Gevers D, Miropolsky L, Garrett WS, et al. Metagenomic biomarker discovery and explanation. *Genome Biol* 2011;12:R60.
 - 28) Brierley J, Gospodarowicz MK, Wittekind C, eds. *TNM Classification of Malignant Tumours*. 8th ed. Chichester, UK; Hoboken, NJ: Wiley Blackwell; 2016.
 - 29) Riquelme E, Zhang Y, Zhang L, Montiel M, Zoltan M, Dong W, et al. Tumor microbiome diversity and composition influence pancreatic cancer outcomes. *Cell* 2019;178:795-806.e12.
 - 30) Vujkovic-Cvijin I, Sklar J, Jiang L, Natarajan L, Knight R, Belkaid Y. Host variables confound gut microbiota studies of human disease. *Nature* 2020;587:448-454.
 - 31) Walter J, Armet AM, Finlay BB, Shanahan F. Establishing or exaggerating causality for the gut microbiome: lessons from human microbiota-associated rodents. *Cell* 2020;180:221-232.
 - 32) Thyagarajan S, Zhang Y, Thapa S, Allen MS, Phillips N, Chaudhary P, et al. Comparative analysis of racial differences in breast tumor microbiome. *Sci Rep* 2020;10:14116.
 - 33) Livyatan I, Nejman D, Shental N, Straussman R. Characterization of the human tumor microbiome reveals tumor-type specific intra-cellular bacteria. *Oncoimmunology* 2020;9:1800957.
 - 34) Ajami NJ, Wargo JA. AI finds microbial signatures in tumours and blood across cancer types. *Nature* 2020;579:502-503.
 - 35) Stower H. Predicting pancreatic cancer survival via the tumor microbiome. *Nat Med* 2019;25:1330.
 - 36) Flores Bueso Y, Walker SP, Hogan G, Claesson MJ, Tangney M. Protoblock - a biological standard for formalin fixed samples. *Microbiome* 2020;8:122.
 - 37) Hooks KB, O'Malley MA. Dysbiosis and its discontents. *MBio* 2017;8:e01492-17.
 - 38) Zhou W, Duan Z, Yang B, Xiao C. The effective regulation of pro- and anti-inflammatory cytokines induced by combination of PA-MSHA and BPIFB1 in initiation of innate immune responses. *Open Med (Wars)* 2017;12:299-307.
 - 39) Yin TQ, Ou-Yang X, Jiao FY, Huang LP, Tang XD, Ren BQ. *Pseudomonas aeruginosa* mannose-sensitive hemagglutinin inhibits proliferation and invasion via the PTEN/AKT pathway in HeLa cells. *Oncotarget*. 2016;7:37121-37131.
 - 40) Zhao X, Wu X, Yu W, Cai X, Liu Q, Fu X, et al. PA-MSHA inhibits proliferation and induces apoptosis in human non-small cell lung cancer cell lines with different genotypes. *Mol Med Rep* 2016;14(6):5369-5376.
 - 41) Cong WM, Wu MC. New insights into molecular diagnostic pathology of primary liver cancer: advances and challenges. *Cancer Lett* 2015;368:14-19.
 - 42) International Agency for Research on Cancer. *Digestive System Tumours. WHO Classification of Tumours*. 5th ed. Vol. 1. Geneva, Switzerland: World Health Organization; 2019.
 - 43) Bosman FT, Carneiro F, Hruban RH, Theise ND, eds. *WHO Classification of Tumours of the Digestive System*. 4th ed. Geneva, Switzerland: World Health Organization; 2010.
 - 44) Nagtegaal ID, Odze RD, Klimstra D, Paradis V, Rugge M, Schirmacher P, et al.; WHO Classification of Tumours Editorial Board. The 2019 WHO classification of tumours of the digestive system. *Histopathology* 2020;76:182-188.
 - 45) Brunt E, Aishima S, Clavien PA, Fowler K, Goodman Z, Gores G, et al. cHCC-CCA: consensus terminology for primary liver carcinomas with both hepatocytic and cholangiocytic differentiation. *Hepatology* 2018;68:113-126.
 - 46) Cazals-Hatem D, Rebouissou S, Bioulac-Sage P, Bluteau O, Blanche H, Franco D, et al. Clinical and molecular analysis of combined hepatocellular-cholangiocarcinomas. *J Hepatol* 2004;41:292-298.

Supporting Information

Additional Supporting Information may be found at onlinelibrary.wiley.com/doi/10.1002/hep4.1908/suppinfo.